Molecular Recognition by the Protonated Hexaaza Macrocyclic Ligand 3,6,9,16,19,22-Hexaaza-27,28-dioxatricyclo[22.2.1.1^{11,14}]octacosa-1(26),11,13,24-tetraene

Qin Lu, Ramunas J. Motekaitis, Joseph J. Reibenspies, and Arthur E. Martell*

Department of Chemistry, Texas A&M University, College Station, Texas 77843-3255

Received April 26, 1995

The hexaaza macrocyclic ligand 3,6,9,16,19,22-hexaaza-27,28-dioxatricyclo[22.2.1.1^{11,14}]octacosa-1(26),11,13,-24-tetraene (BFBD), prepared via 2+2 condensation of 2,5-diformylfuran with diethylenetriamine, followed by reduction with NaBH$_4$, forms a variety of cationic species including mono- through hexaprotonated forms of the macrocycle in aqueous solution. These cationic hosts recognize certain substrates such as oxalate, malonate, and pyrophosphate anions. Formation constants measuring this recognition are reported for all species found from the potentiometric studies and are compared with those of the analogous ligand 1,4,7,13,16,19-hexaaza-10,22-dioxacyclotetracosane (OBISDIEN). Two binary complexes (H$_6$BFBD-C$_2$O$_4$)Cl$_4$·4H$_2$O, **1**, and (H$_5$BFBD-H$_2$P$_2$O$_7$)-Cl$_3$·5H$_2$O, **2**, have been characterized by single-crystal X-ray diffraction. Complex **1** crystallizes in the monoclinic system, space group P2$_1$/n, with a = 6.2630(10) Å, b = 19.682(3) Å, c = 13.870(2) Å, β = 91.210(10)°, and Z = 2, and complex **2** crystallizes in the triclinic system, space group P1̄, with a = 12.675(5) Å, b = 12.792(5) Å, c = 12.868(5) Å, α = 97.44(3)°, β = 115.03(3)°, γ = 105.40(3)°, and Z = 2. The X-ray crystal structure results reveal that the binding of anionic substrates to protonated BFBD is through hydrogen bonds between negatively charged oxygens of the substrates and protonated, positively charged amino nitrogens of BFBD.

Introduction

It has been shown that macrocyclic polyamines have numerous advantages as enzyme models. They are capable of undergoing polyprotonation in solution, forming positively charged polyammonium cations which can bind selectively a variety of inorganic, organic, and biologically important anions, *via* electrostatic forces and hydrogen bonding.[1−9] The cavity size of the macrocycles can be readily varied, and both alkyl and aromatic groups can be incorporated into macrocycles during the synthetic process, which allows for the construction of macrocycles with varying charge densities and flexibilities.[10−15]

The macrocyclic hexaamine ligand 3,6,9,16,19,22-hexaaza-27,28-dioxatricyclo[22.2.1.1^{11,14}]octacosa-1(26),11,13,24-tet-

Chart 1

1 BFBD

2 Possible H-bonding modes in H$_4$BfOx^{2+}

3 Possible H-bonding modes in H$_6$BfMal^{4+}

4 Possible H-bonding modes in H$_4$BfPp
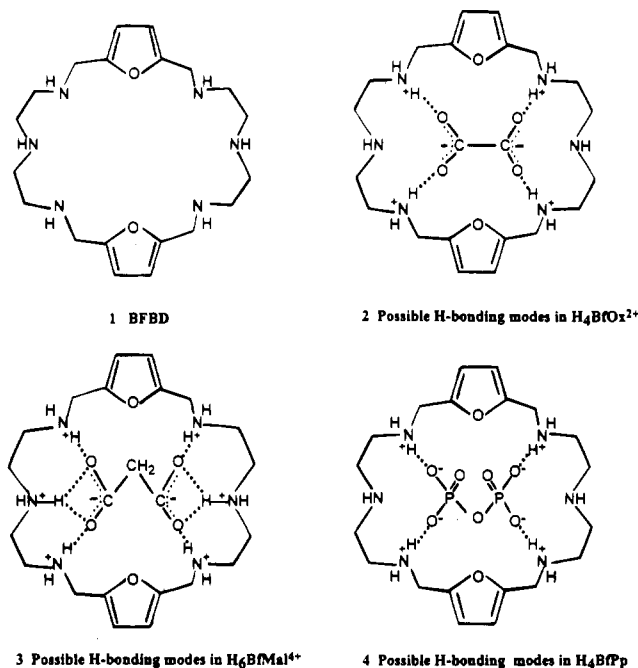
raene (BFBD), an analog of OBISDIEN,[10] is such a bis-chelating macrocycle that contains two diethylenetriamine units separated by two five-atom bridges (formula **1**, Chart 1). The central atoms of these two bridges are furan oxygen atoms instead of the aliphatic ether oxygen atoms as in OBISDIEN. Thus this macrocyclic ligand will have some rigidity due to the incorporation of two aromatic rings. We report here the potentiometric equilibrium studies and molecular recognition of oxalate, malonate, and pyrophosphate anions by protonated BFBD. The crystal structures of the binary complexes (H$_6$BFBD-C$_2$O$_4$)Cl$_4$·4H$_2$O, **1**, and (H$_5$BFBD-H$_2$P$_2$O$_7$)Cl$_3$·5H$_2$O, **2**, are also described.

® Abstract published in *Advance ACS Abstracts*, September 1, 1995.

(1) Simmons, H. E.; Park, C. H. *J. Am. Chem. Soc.* **1968**, *90*, 2428.
(2) Graf, E.; Lehn, J. M. *J. Am. Chem. Soc.* **1976**, *98*, 6403.
(3) Manfrin, M. F.; Maggi, L.; Castelvetro, V.; Balzani, V.; Hosseini, M. W.; Lehn, J. M. *J. Am. Chem. Soc.* **1985**, *107*, 6888.
(4) Hosseini, M. W.; Lehn, J. M. *Helv. Chim. Acta* **1986**, *69*, 587.
(5) Hosseini, M. W.; Lehn, J. M. *Helv. Chim. Acta* **1988**, *71*, 749.
(6) Motekaitis, R. J.; Martell, A. E. *Inorg. Chem.* **1992**, *31*, 5534.
(7) Bencini, A.; Bianchi, A.; Dapporto, P.; Garcia-España, E.; Micheloni, M.; Ramirez, J. A.; Paoletti, P.; Paoli, P. *Inorg. Chem.* **1992**, *31*, 1902.
(8) Andres, A.; Bazzicalupi, C.; Bencini, A.; Bianchi, A.; Fusi, V.; Garcia-España, E.; Giorgi, C.; Nardi, N.; Paoletti, P.; Ramirez, J. A.; Valtancoli, B. *J. Chem. Soc., Perkin Trans. 2* **1994**, 2367.
(9) Bencini, A.; Bianchi, A.; Burguete, M. I.; Dapporto, P.; Doménech, A.; Garcia-Espana, E.; Luis, S. V.; Paoli, P.; Ramirez, J. A. *J. Chem. Soc., Perkin Trans. 2* **1994**, 569.
(10) Lehn, J. M.; Pine, S. H.; Watanabe, E.; Willard, A. K. J. *J. Am. Chem. Soc.* **1977**, *99*, 6766.
(11) Mertes, K. B.; Lehn, J. M. In *Comprehensive Coordination Chemistry*; Wilkinson, G., Ed.; Pergamon Press: New York, 1987.
(12) Agnus, Y. L. In *Copper Coordination Chemistry: Biochemical and Inorganic Perspectives*; Karlin, K. D., Zubieta, J., Eds.; Adenine Press: New York, 1983.
(13) Martin, A. E.; Lippard, S. J. In *Copper Coordination Chemistry: Biochemical and Inorganic Perspectives*; Karlin, K. D., Zubieta, J., Eds.; Adenine Press: New York, 1983.
(14) Lehn, J. M. *Angew. Chem., Int. Ed. Engl.* **1988**, *27*, 89.
(15) Martell, A. E. In *Crown Compounds: Toward Future Applications*; Copper, S. R., Ed.; VCH: New York, 1992.

Experimental Section

Materials. GR grade KCl was obtained from EM Chemical Co., CO_2-free Dilut-it ampules of KOH were obtained from J. T. Baker Inc., and reagent grade oxalic acid was purchased from Fisher Scientific Co.

Reagent grade tetrasodium pyrophosphate from Fisher Scientific Co. and malonic acid from Aldrich Chemical Co. were purified by recrystallization from distilled water.

The KOH solution was standardized by titration with potassium acid phthalate, and the extent of carbonate accumulation was checked periodically by titration with a standard hydrochloric acid solution.

Potentiometric Measurements. All p[H] calibrations were performed with standard dilute strong acid at 0.10 M ionic strength (KCl) in order to measure hydrogen ion concentration directly. Thus p[H] is defined as $-\log$ [H$^+$].

Potentiometric studies of BFBD in the absence and presence of anionic substrates were carried out with a Corning Model 350 pH meter filled with blue-glass and calomel reference electrodes. Each aqueous system under consideration was measured in a 50 mL jacketed cell thermostated at 25.0 $\pm$ 0.05 °C by a mechanically refrigerated circulating water bath. The ionic strength was adjusted to 0.10 M by the addition of KCl as supporting electrolyte. The concentrations of all the experimental solutions were approximately 2×10^{-3} M. The stoichiometry of BFBD—substrate systems is 1:1. All systems were studied under anaerobic conditions, established by a stream of prepurified nitrogen. Experimental runs were carried out by adding increments of standard base to a solution containing the acid (hexahydrochloride) form of the macrocycle plus other components. Each p[H] profile was determined by two titrations, and each titration was determined by utilizing at least 10 points per neutralization of 1 hydrogen ion equiv. The range of accurate p[H] measurements was considered to be 2−12. In all potentiometric determinations the σ_{fit},[16] which measures the deviation between the measured pH values and the pH values calculated from the equilibrium constants, was less than 0.01 pH unit. A variation in log K of 0.01−0.015 was required to produce an observable deviation in the distribution curves. In view of other experimental uncertainties such as the weight of the sample and the volume of the titrant, the error in the constants listed in Tables 1−5 is estimated as $\pm$0.02 log unit.

Calculations. Equilibrium constants were calculated with the program BEST.[16] The log K_w for the system, defined in terms of log [H$^+$][OH$^-$], was found to be -13.78 at the ionic strength employed and was maintained fixed during refinements. Species distribution diagrams were computed from the equilibrium constants with the help of the program SPE and plotted on a laser Jet with SPEPLOT. Details of the potentiometric method have been discussed.[16]

Preparation of Crystalline Complexes for X-ray Analysis. The ligand BFBD was prepared as a colorless crystalline hexahydrochloride by the method previously described.[17]

Binary complex 1, BFBD·6HCl (0.300 mmol), and 0.300 mmol of $Na_2C_2O_4$ were mixed in water, followed by slow ethanol diffusion at room temperature. Colorless platelike crystals suitable for X-ray analysis were formed in about a week.

Binary complex 2, BFBD·6HCl (0.300 mmol), and 0.300 mmol of $Na_4P_2O_7$ were dissolved in water, and the p[H] of the resulting solution was adjusted to $\sim$3.5 with 0.10 M HCl solution. After several days of ethanol diffusion into the solution, colorless needlelike crystals were collected for X-ray analysis.

Crystal Structure Determination. A colorless plate of **1** or a colorless needle of **2** was mounted on a glass fiber with epoxy cement. Preliminary examination and data collection were performed with an AFC5R Rigaku single-crystal X-ray diffractometer (oriented graphite monochromator, Mo Kα λ = 0.710 73 Å radiation) at 163(2) K. Cell parameters were calculated from the least-squares fit for 25 high-angle reflections ($2\theta > 15°$). ω scans for several intense reflections indicated acceptable crystal quality.

Data were collected for $5.08 \leq 2\theta \leq 50.16°$ for **1** and $5.04 \leq 2\theta \leq 50.20°$ for **2** at 163(2) K. Scan widths for data collection were [1.47

Table 1. Overall and Stepwise Protonation Constants of BFBD and OBISDIEN (μ = 0.10 M (KCl), 25.0 °C; Bf = BFBD, H = H$^+$)

stoichiometry				log K	
Bf	H	log β^a	stepwise constant, K	BFBD^a	OBISDIEN
1	1	9.44	[BfH]/[Bf][H]	9.44	9.65
1	2	18.12	[BfH$_2$]/[BfH][H]	8.68	8.92
1	3	25.75	[BfH$_3$]/[BfH$_2$][H]	7.63	8.30
1	4	32.21	[BfH$_4$]/[BfH$_3$][H]	6.46	7.64
1	5	36.05	[BfH$_5$]/[BfH$_4$][H]	3.84	3.81
1	6	39.23	[BfH$_6$]/[BfH$_5$][H]	3.18	3.26

^{a} Estimated error = $\pm$0.02.

Table 2. Stepwise Protonation Constants of Substrates^a (μ = 0.10 M (KCl), 25.0 °C)

substrate	log K_1	log K_2	log K_3
oxalate	3.86^b (3.83)	(1.0)	
malonate	5.29^b (5.28)	2.60^b (2.63)	
pyrophosphate	8.55^b (8.40)	6.09^b (6.03)	2.07^b (1.9)

^{a} Values in parentheses are literature values. ^{b} Estimated error = $\pm$0.02.

Table 3. Overall Stability Constants and Stepwise Formation Constants for the Interaction of BFBD with Oxalate (μ = 0.10 M (KCl), 25.0 °C; Bf = BFBD, Ox = Oxalate(2−), H = H$^+$)

stoichiometry					
Bf	Ox	H	log β^a	quotient K	log K^a
1	1	4	35.18	[BfOxH$_4$]/[BfH$_4$][Ox]	2.97
1	1	5	40.17	[BfOxH$_5$]/[BfH$_5$][Ox]	4.12
1	1	6	44.20	[BfOxH$_6$]/[BfH$_6$][Ox]	4.97

^{a} Estimated error = $\pm$0.02.

+ 0.3 tan(θ)]° for **1** and [1.54 + 0.3 tan(θ)]° for **2** in ω with a variable scan rate between 4 and 16° min^{-1}. Weak reflections were rescanned (maximum of two rescans), and the counts for each scan were accumulated. The three standards, collected every 150 reflections, showed no significant trends. Background measurement was made by the stationary-crystal/stationary-counter technique at the beginning and the end of each scan for half of the total scan time.

Lorentz and polarization corrections were applied to 2979 reflections for **1** and 6403 reflections for **2**. A semiempirical absorption correction was applied. The structure was solved by direct methods.[18] Full-matrix least-squares anisotropic refinement[19] of all non-hydrogen atoms yielded $R = 0.049$ for **1** and $R = 0.066$ for **2** at convergence. Hydrogen atoms were placed in idealized positions with isotropic thermal parameters fixed at 0.08 Å^2. Neutral atom scattering factors and anomalous scattering factors were taken from ref 20.

Results and Discussion

Protonation Constants of BFBD. In the absence of added anionic substrate, the potentiometric equilibrium curve of BFBD·6HCl was found to possess an inflection at a = 2 (where a = mol of base added/mol of ligand), which corresponds to the completion of the neutralization of the two most acidic ammonium ions. The buffer region occurring at higher p[H] corresponds to the neutralization of the remaining four ammonium groups of the ligand in sequential overlapping steps.

(16) Martell, A. E.; Motekaitis, R. J. *Determination and Use of Stability Constants*, 2nd ed.; VCH: New York, 1989.
(17) Chen, D.; Martell, A. E. *Tetrahedron* **1991**, *34*, 6895.

(18) Sheldrick, G. M. SHELXS-86: Program for Crystal Structure Solution. Institute für Anorganische Chemie der Universität, Göttingen, Germany.
(19) Sheldrick, G. M. SHELXS-93: Program for Crystal Structure Refinement. Institute für Anorganishe Chemie der Universität, Göttingen, Germany.
(20) Hahn, T. Ed. *International Tables for X-Ray Crystallography*; Reidel: Dordrecht, The Netherlands, 1992; Vol. C.

Figure 1. Species distribution diagram showing the species formed as a function of p[H] when 2×10^{-3} M each BFBD and oxalate anion are equilibrated at 25.0 °C, $\mu = 0.1$ M (KCl). Only the BFBD-containing species are shown.

For purpose of comparison, Table 1 lists the log values of the protonation constants for both BFBD and its analog OBISDIEN.[21]

It is noted from Table 1 that the overall log protonation constant, $\sum \log K_i^H$ of BFBD is 39.23, which is more than 2 log units less than that of OBISDIEN, 41.58. The lower overall basicity of BFBD relative to that of OBISDIEN may be due to the fact that BFBD contains two furan oxygen atoms instead of ether oxygen atoms. These two furan oxygen atoms withdraw electron density more strongly from nearby amino groups, resulting in K_3^H and K_4^H being 0.67 and 1.18 log units less than the corresponding values of OBISDIEN.

Protonation Constants of Substrates. In preparation for the quantitative determination of the stability constants of substrates with protonated forms of the macrocycle BFBD, protonation constants of substrates have been determined separately under the conditions of these experiments. The protonation constants obtained for oxalate, malonate, and pyrophosphate anions are listed in Table 2. The literature values of protonation constants of these substrates[22] are also listed in Table 2.

Binding of the Oxalate Anion by Protonated BFBD. The equilibrium constants obtained for the binding of the oxalate anion to BFBD are shown in Table 3. Potentiometric data indicate that only the tetra-, penta-, and hexaprotonated forms of BFBD bind the oxalate anion, and the strength of binding decreases as the number of protonated nitrogens is decreased from the maximum value of 6 to 4, below which oxalate binding is too weak to be detected. The species distribution diagram of the BFBD—oxalate system (Figure 1) shows the hexaprotonated species H_6BfOx^{4+} to be the predominant species between pH 2 and 4. At higher p[H], where BFBD is less protonated,

Table 4. Overall Stability Constants and Stepwise Formation Constants for the Interaction of BFBD with Malonate ($\mu = 0.10$ M (KCl), 25.0 °C; Bf = BFBD, Mal = Malonate(2−), H = H⁺)

stoichiometry					
Bf	Mal	H	$\log \beta^a$	quotient K	$\log K^a$
1	1	4	34.31	$[BfMalH_4]/[BfH_4][Mal]$	2.10
1	1	5	39.44	$[BfMalH_5]/[BfH_5][Mal]$	3.39
1	1	6	43.24	$[BfMalH_6]/[BfH_6][Mal]$	4.01
1	1	7	46.38	$[BfMalH_7]/[BfH_6][MalH]$	1.86

^{a} Estimated error = ±0.02.

the penta- and tetraprotonated species, H_5BfOx^{3+} and H_4BfOx^{2+}, form at somewhat lower concentration and disappear completely above pH 8.

In comparison of the above results with those obtained from OBISDIEN,[23] the protonated BFBD binds the oxalate anion more strongly. This better recognition may be due to the more rigid structure of BFBD arising from the two aromatic rings in the macrocycle, which can accommodate the small oxalate anion more comfortably than the very flexible macrocycle OBISDIEN. It is suggested that the binding of oxalate to protonated BFBD must be through hydrogen bonding to the protonated, positively charged amino groups of the macrocycle, formula **2** (Chart 1). This type of bonding is the same as has been reported for the hexaaza macrocycle OBISDIEN, and the complexes formed probably have similar structures.

Binding of the Malonate Anion by Protonated BFBD. Table 4 lists the equilibrium constants obtained for the BFBD— malonate systems. It is seen that as the degree of protonation on BFBD increases, its affinity for the malonate anion increases. However there are additional factors which determine the relative concentrations of these various protonated binary species, because p[H] affects the degree of protonation of malonate as well as that of BFBD. When p[H] is lowered to 2, BFBD is in its maximum protonated state (hexaprotonated) and malonate is actually all H_2Mal. Obviously there is no

(21) Motekaitis, R. J.; Martell, A. E.; Lecomte, J. P.; Lehn, J. M. *Inorg. Chem.* **1983**, *22*, 609.

(22) Martell, A. E.; Smith, R. M.; Motekaitis, R. J. *NIST Critical Stability Constants of Metal Complexes Database 46*; NIST: Gaithersburg, MD, 1993.

(23) Motekaitis, R. J.; Martell, A. E. *J. Am. Chem. Soc.* **1988**, *110*, 8059.
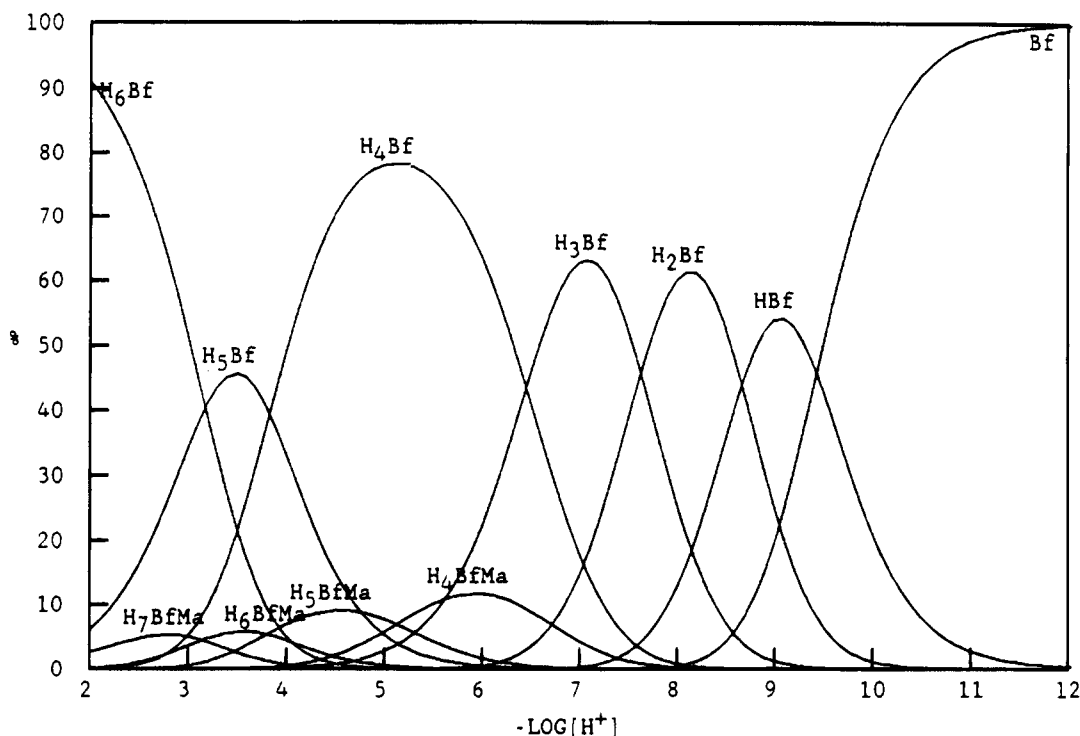
Figure 2. Species distribution diagram showing the species formed as a function of p[H] when 2×10^{-3} M each BFBD and malonate anion are equilibrated at 25.0 °C, $\mu = 0.1$ M (KCl). Only the BFBD-containing species are shown.

Table 5. Overall Stability Constants and Stepwise Formation Constants for the Interaction of BFBD with Pyrophosphate ($\mu = 0.10$ M (KCl), 25.0 °C; Bf = BFBD, Pp = Pyrophosphate(4−), H = H$^+$)

Bf	Pp	H	log β^a	quotient K	log K^a	principal equilibrium K'	log K' ^{a}
	stoichiometry						
1	1	1	11.64	[BfPpH]/[BfH][Pp]	2.20	[BfPpH]/[BfH][Pp]	2.20
1	1	2	20.73	[BfPpH$_2$]/[BfH$_2$][Pp]	2.61	[BfPpH$_2$]/[BfH$_2$][Pp]	2.61
1	1	3	29.12	[BfPpH$_3$]/[BfH$_3$][Pp]	3.37	[BfPpH$_3$]/[BfH$_2$][PpH]	2.45
1	1	4	37.91	[BfPpH$_4$]/[BfH$_4$][Pp]	5.70	[BfPpH$_4$]/[BfH$_3$][PpH]	3.61
1	1	5	45.58	[BfPpH$_5$]/[BfH$_5$][Pp]	9.53	[BfPpH$_5$]/[BfH$_4$][PpH]	4.82
1	1	6	51.78	[BfPpH$_6$]/[BfH$_6$][Pp]	12.55	[BfPpH$_6$]/[BfH$_4$][PpH$_2$]	4.93
1	1	7	56.26	[BfPpH$_7$]/[BfH$_6$][PpH]	8.48	[BfPpH$_7$]/[BfH$_5$][PpH$_2$]	5.57
1	1	8	58.40	[BfPpH$_8$]/[BfH$_6$][PpH$_2$]	4.53	[BfPpH$_8$]/[BfH$_6$][PpH$_2$]	4.53

^{a} Estimated error = ± 0.02.

interaction between these two species at this p[H]. When the p[H] is increased, HMal$^-$ and Mal^{2-} become the major forms of malonate sequentially and can bind to protonated BFBD to form H$_x$BfMal$^{(x-2)+}$. It is seen from the species distribution diagram of the BFBD−malonate system (Figure 2) that, at p[H] 2.8, 3.5, 4.6, and 6, H$_7$BfMal^{5+}, H$_6$BfMal^{4+}, H$_5$BfMal^{3+}, and H$_4$BfMal^{2+} reach their maximum concentrations successively. None of these binary species exist as major species in the region p[H] 2−8, nor are they negligible. Above p[H] 8, binary species are not detected and probably do not exist in measurable concentrations.

The weaker binding of the malonate anion by protonated BFBD as compared with that of the oxalate anion has also been reported for the OBISDIEN−malonate system.[24] The fact that the malonate anion is more basic than the oxalate anion would tend to make it more strongly bound. The effect from the poorer structural matching between the host and guest prevails over that from the basicity, and the binding of the malonate anion by protonated BFBD is much weaker than the bonding between the oxalate anion and the same ligand. The possible mode for hydrogen-bonding of the malonate anion to protonated BFBD is illustrated by formula **3** (Chart 1).

Binding of Pyrophosphate by Protonated BFBD. The stability constants for the BFBD−pyrophosphate complexes have been determined and are presented in Table 5. It is found that a variety of binary species, including mono- to octaprotonated species, form through the binding of pyrophosphate by protonated BFBD. Figure 3 shows the species distribution diagram obtained for the BFBD−pyrophosphate system. Below p[H] 8, five species from H$_8$BfPp^{4+} through H$_4$BfPp are the predominant complexes, while above p[H] 8, where BFBD is less protonated, the remaining three species H$_3$BfPp$^-$, H$_2$BfPp^{2-}, and HBfPp^{3-} are formed as minor species.

Judging from the log protonation constants of the pyrophosphate anion (8.56, 6.09, and 2.09), two protonated forms of the pyrophosphate anion, H$_2$P$_2$O$_7$$^{2-}$ and HP$_2$O$_7$$^{3-}$, are important between p[H] 2 and 10. Considering both protonation constants of BFBD and the pyrophosphate anion, the main species formed in the p[H] range 2−6 are actually H$_6$Bf-H$_2$Pp^{4+}, H$_5$Bf-H$_2$Pp^{3+}, and H$_4$Bf-H$_2$Pp^{2+}. Similarly, the species H$_4$BfPp and H$_3$BfPp$^-$ can be described as H$_3$Bf-HPp and H$_2$Bf-HPp$^-$. The principal equilibria and equilibrium constants are also listed in Table 5.

The formation constants obtained for this system are comparable with those previously reported for the OBISDIEN−

(24) Motekaitis, R. J.; Martell, A. E. *Inorg. Chem.* **1992**, *31*, 5534.
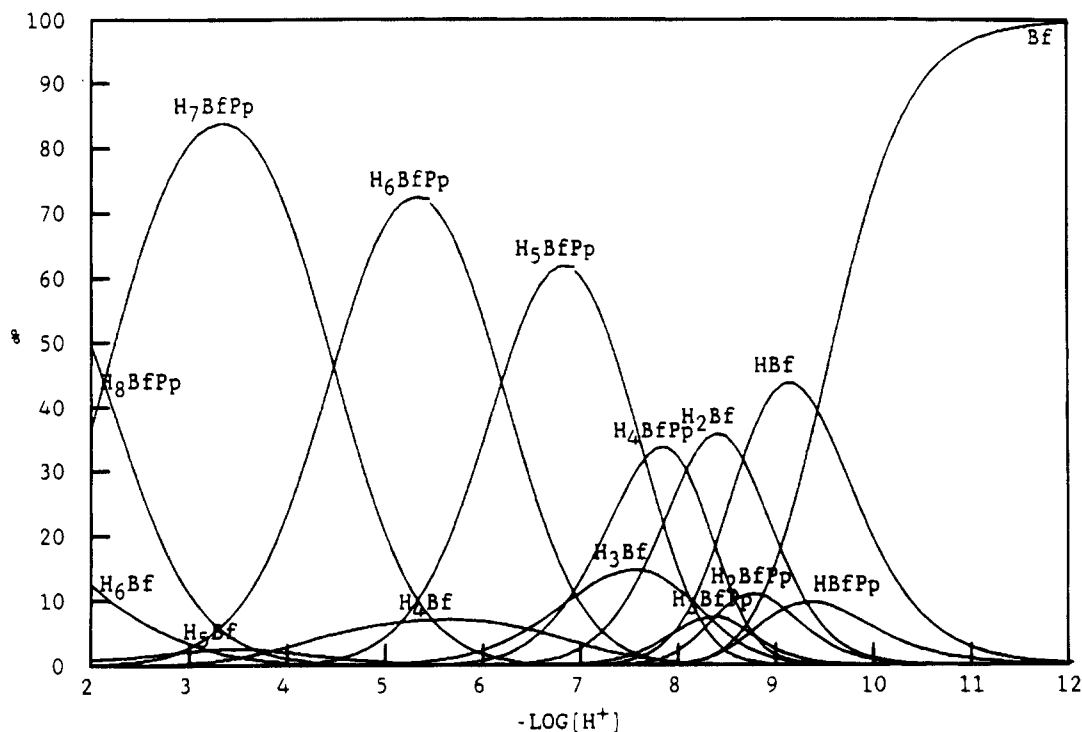
Figure 3. Species distribution diagram showing the species formed as a function of p[H] when 2×10^{-3} M each BFBD and pyrophosphate anion are equilibrated at 25.0 °C, $\mu = 0.1$ M (KCl). Only the BFBD-containing species are shown.
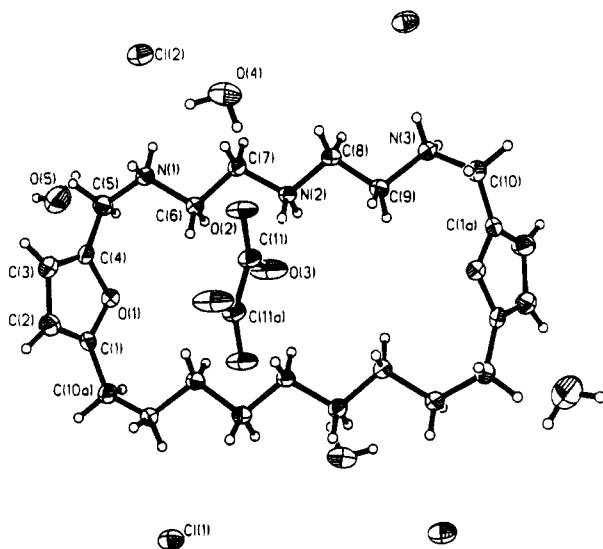
Figure 4. ORTEP drawing of complex **1**, 50% probability, with atomic labeling.

pyrophosphate system.[25] It is clear that the pyrophosphate anion has more hydrogen-binding sites and is much more basic than oxalate and malonate anions and is thus the substrate with the highest formation constants among the three substrates discussed in this paper. The suggested hydrogen-bonding of the pyrophosphate anion by protonated BFBD is given in formula **4** (Chart 1).

Crystal Structure of Binary Complex 1. Figure 4 shows an ORTEP drawing of the binary complex **1** with the atom-labeling scheme. A summary of crystallographic results is given in Table 6. Atomic coordinates and bond lengths and angles are given in Tables 7 and 8. The hexaprotonated macrocyclic ligand H_6BFBD^{6+} adopts a "chair" conformation with the three nitrogen atoms of each diethylenetriamine unit linearly accom-

(25) Jurek, P. E.; Martell, A. E.; Motekatis, R. J.; Hancock, R. D. *Inorg. Chem.* **1995**, *34*, 1823.

Table 6. Crystal Data for H_6BfBD-C_2O_4 (**1**) and H_5BfBD-$H_2P_2O_7$ (**2**)

	complex **1**	complex **2**
formula	$C_{22}H_{48}Cl_4N_6O_{10}$	$C_{20}H_{50}Cl_3N_6O_{14}P_2$
fw	698.46	766.95
space group	$P2_1/n$	$P\bar{1}$
a, Å	6.263(1)	12.675(5)
b, Å	19.682(3)	12.792(5)
c, Å	13.870(2)	12.868(5)
α, deg		97.44(3)
β, deg	91.210(1)	115.03(3)
γ, deg		105.40(3)
V, Å³	1709.4(5)	1751.3(1)
Z	2	2
d_{calc}, g/cm³	1.357	1.545
radiation	Mo Kα (0.710 73 Å)	Mo Kα (0.710 73 Å)
μ, mm⁻¹	0.402	0.421
temp, K	163(2)	163(2)
$F(000)$	740	810
R^a	0.049	0.066
R_w^b	0.123	0.140

$^a R = \Sigma||F_o| - |F_c||/\Sigma|F_o|$. $^b R_w = (\Sigma w(F_o^2 - F_c^2)^2)^{1/2}$. $w^{-1} = \sigma^2(F^2)$ $+ (x(F_o^2 + 2F_c^2)/3)^2 + y(F_o^2 + 2F_c^2)/3$. $x = 0.06, y = 1.94$ for complex **1**; $x = 0.064, y = 0.00$ for complex **2**.

modated in a plane which contains the rest of the aliphatic carbons, while the two furan rings point in opposite directions. The intramolecular distances between symmetry-related nitrogen atoms are 6.08, 4.60, and 6.08 Å, while the intramolecular distance between two furan oxygen atoms is 9.72 Å. The oxalate anion binds to H_6BFBD^{6+} through hydrogen bonds. One of the oxygen atoms from one of the carboxylic acid groups forms two hydrogen bonds simultaneously with two central nitrogen atoms of both diethylenetriamine units (O(3)−N(2), 2.65 Å; O(3)−N(2a), 2.83 Å), while another oxygen atom from the second carboxylic acid group forms a hydrogen bond with one of the central nitrogen atoms of a diethylenetriamine unit (O(2)−N(2), 2.75 Å). The remaining two oxygen atoms of the oxalate anion are also hydrogen-bonded to another protonated macrocyclic ligand in the same pattern. These N−H⁺···O⁻

Table 7. Atomic Coordinates ($\times 10^4$) and Equivalent Isotropic Displacement Parameters ($\text{Å}^2 \times 10^3$) for **1**

	x	y	z	$U(\text{eq})^a$
Cl(1)	−181(1)	7984(1)	2786(1)	34(1)
Cl(2)	497(1)	1746(1)	2306(1)	35(1)
O(1)	431(3)	4820(1)	3493(2)	25(1)
O(2)	−5076(3)	4125(1)	−184(2)	35(1)
O(3)	−2304(3)	4821(1)	−70(2)	47(1)
O(4)	−4449(4)	2716(1)	−46(2)	46(1)
O(5)	4001(5)	3276(2)	5082(2)	61(1)
N(1)	10(4)	3330(1)	2425(2)	24(1)
N(2)	620(4)	3852(1)	−145(2)	20(1)
N(3)	659(4)	3603(1)	−2810(2)	24(1)
C(1)	−870(5)	5337(2)	3777(2)	26(1)
C(2)	−2726(6)	5086(2)	4086(3)	37(1)
C(3)	−2588(6)	4364(2)	3997(2)	34(1)
C(4)	−671(5)	4228(2)	3641(2)	26(1)
C(5)	472(6)	3593(2)	3421(2)	30(1)
C(6)	541(5)	3802(2)	1628(2)	23(1)
C(7)	387(5)	3402(2)	697(2)	23(1)
C(8)	507(5)	3477(2)	−1065(2)	23(1)
C(9)	329(5)	3976(2)	−1892(2)	24(1)
C(10)	−38(5)	3968(2)	−3706(2)	28(1)
C(11)	−4247(5)	4694(2)	−73(2)	24(1)

^{a} $U(\text{eq})$ is defined as one-third of the trace of the orthogonalized $\mathbf{U}_{ij}$ tensor.

Table 8. Bond Lengths (Å) and Angles (deg) for **1**^{a}

O(1)−C(1)	1.365(4)	N(3)−C(10)	1.493(4)
O(1)−C(4)	1.373(4)	C(1)−C(2)	1.342(5)
O(2)−C(11)	1.242(4)	C(1)−C(10)^i	1.485(4)
O(3)−C(11)	1.242(4)	C(2)−C(3)	1.428(5)
N(1)−C(6)	1.487(4)	C(3)−C(4)	1.335(5)
N(1)−C(5)	1.498(4)	C(4)−C(5)	1.476(4)
N(2)−C(8)	1.474(4)	C(6)−C(7)	1.514(4)
N(2)−C(7)	1.475(4)	C(8)−C(9)	1.512(4)
N(3)−C(9)	1.487(4)	C(10)−C(1)^i	485(4)
		C(11)−C(11)^{ii}	1.547(6)
C(1)−O(1)−C(4)	106.6(2)	C(3)−C(4)−C(5)	133.7(3)
C(6)−N(1)−C(5)	115.3(2)	O(1)−C(4)−C(5)	116.2(3)
C(8)−N(2)−C(7)	112.4(2)	C(4)−C(5)−N(1)	113.5(2)
C(9)−N(3)−C(10)	115.5(2)	N(1)−C(6)−C(7)	107.3(2)
C(2)−C(1)−O(1)	110.1(3)	N(2)−C(7)−C(6)	110.9(2)
C(2)−C(1)−C(10)^i	134.1(3)	N(2)−C(8)−C(9)	109.5(2)
O(1)−C(1)−C(10)^i	115.8(3)	N(3)−C(9)−C(8)	108.6(2)
C(1)−C(2)−C(3)	106.5(3)	C(10)^i−C(10)−N(3)	113.1(2)
C(4)−C(3)−C(2)	106.8(3)	O(2)−C(11)−O(3)	126.1(3)
C(3)−C(4)−O(1)	110.0(3)	O(2)−C(11)−C(11)^{ii}	117.7(3)
		O(3)−C(11)−C(11)^{ii}	116.3(3)

^{a} Symmetry transformations used to generate equivalent atoms: $-x$, $-y + 1$, $-z$; $-x - 1$, $-y + 1$, $-z$.

distances correspond to strong hydrogen bonds.[26] Oxalate anions are located above and below the macrocyclic plane instead of being encapsulated inside the macrocycle cavity and form intermolecular hydrogen bonds to macrocycles.

Crystal Structure of Binary Complex 2. Figure 5 illustrates the structure and geometry of the pyrophosphate anion bound to the macrocycle. A summary of crystallographic results is given in Table 6. Atomic coordinates and bond lengths and angles are given in Tables 9 and 10. Table 11 shows the selected distances between hydrogen-bond-related atoms. The structure reveals that the pyrophosphate anion binds to BFBD through multiple hydrogen bonds with one end of the substrate inserting into the macrocycle while the other end extends outside it. The PO_3^{2-} groups of the pyrophosphate anion take an almost overlapping conformation about the P−P axis with a POP angle

(26) Lehn, M. M.; Merec, R.; Vigneron, J. P.; Bkouche-Waksman, I.; Pascard, C. *J. Chem. Soc., Chem. Commun.* **1991**, 62.
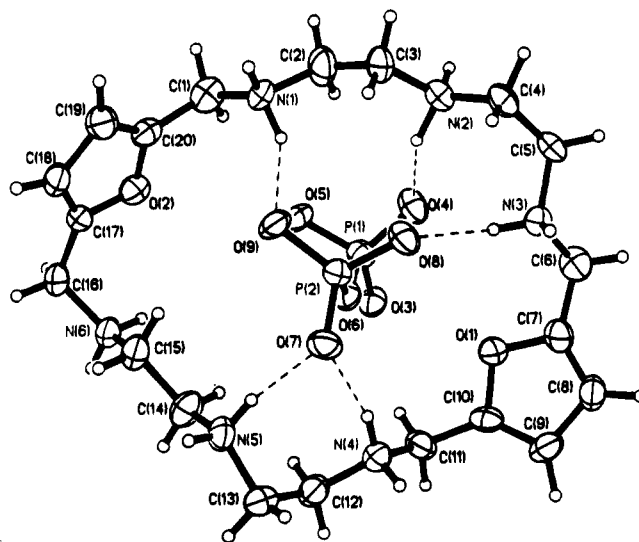
Figure 5. Structure and geometry of the complex **2** cation with atomic labeling.

of 131.3(3)°, close to the value of 134.3(1)° found in the structure of putrescinium dihydrogen diphosphate.[27] It is seen from Figure 5 and Table 11 that three oxygen atoms of the "inside" PO_3^{2-} group and one oxygen from the "outside" PO_3^{2-} form hydrogen bonds to the macrocycle while the remaining two oxygen atoms of the "outside" PO_3^{2-} form hydrogen bonds to two oxygen atoms of pyrophosphate from another macrocycle−substrate binary complex. The hydrogen-bond-related O- -N distances fall in the range of medium to strong hydrogen bonds (2.64−2.81 Å). However, O(8)- -N3, which is much longer (2.93 Å), must involve a weaker hydrogen bond. Taking into account the difference in properties of the $R_2NH_2^+$ proton and OH proton donors, it is suggested that the longest O(8)- -N3 distance arises from the weak hydrogen bond between the O−H proton donor of pyrophosphate anion and R_2N−H proton acceptor of the macrocycle, while others form through $R_2NH_2^+$ proton donors and O^- proton acceptors. The pyrophosphate anion is actually biprotonated to have two OH donors with one OH donor forming a hydrogen bond to the macrocycle while the second one forms a hydrogen bond with another pyrophosphate. Therefore this macrocycle−substrate binary complex can be formulated as $H_5Bf\text{-}H_2P_2O_7^{3+}$. This interpretation is also supported by evidence from potentiometric measurements. At pH ~3.5, at which the crystals were isolated, the major species in solution is $H_5Bf\text{-}H_2P_2O_7^{3+}$.

The geometry of the macrocyclic ligand in this binary complex is different from the one in complex **1**. In this case, the macrocycle adopts a bowl conformation instead a chair configuration. Three of four N−C−C−N torsion angles are of the *gauche* type, while one is in the *trans* conformation. The intramolecular distance between central nitrogen atoms is lengthened to 7.96 Å while the distance between furan oxygen atoms is shortened to 8.06 Å. The large deviation of the conformation of BFBD in complex **2** from that in complex **1** may be explained in terms of different modes of complexation of the anions by the protonated macrocycle. In complex **1**, the oxalate anion forms hydrogen bonds with protonated BFBD in a way which does not affect the conformation of BFBD itself very much. In complex **2**, protonated BFBD adopts a bowl conformation in order to include the pyrophosphate anion in its cavity.

(27) Bartoszak, E.; Jaskólski, M. *Acta Crystallogr.* **1990**, *C46*, 2158.

Table 9. Atomic Coordinates ($\times 10^4$) and Equivalent Isotropic Displacement Parameters ($\text{Å}^2 \times 10^3$) for **2**

	x	y	z	$U(\text{eq})^a$
Cl(1)	1955(2)	6280(2)	5951(2)	64(1)
Cl(2)	−5743(2)	1818(2)	−2095(3)	73(1)
Cl(3)	5000	5000	0	64(1)
P(1)	−862(2)	1095(2)	−475(2)	36(1)
P(2)	853(2)	3230(2)	1386(2)	32(1)
O(1)	281(5)	2862(5)	−1934(5)	42(2)
O(2)	94(5)	467(5)	3505(5)	43(2)
O(3)	−640(5)	369(5)	−1328(5)	40(2)
O(4)	−1859(5)	1568(5)	−1028(5)	45(2)
O(5)	−1143(5)	414(4)	388(5)	41(2)
O(6)	460(5)	2085(4)	380(4)	34(1)
O(7)	2248(5)	3737(4)	1794(5)	40(2)
O(8)	131(5)	3914(5)	757(5)	40(2)
O(9)	565(5)	2877(5)	2350(5)	41(2)
O(10)	2345(5)	4209(5)	4665(5)	57(2)
O(11)	5733(5)	4029(6)	5258(5)	70(2)
O(12)	−5600(6)	3947(6)	−3446(6)	78(2)
O(13)	−4650(10)	−179(8)	−1633(10)	170(5)
O(14)	3463(12)	8512(10)	5904(12)	221(6)
O(15)	4291(5)	−833(4)	4030(5)	85(3)
N(1)	−1634(6)	2055(6)	2351(5)	37(2)
N(2)	−2924(6)	2883(6)	−327(6)	43(2)
N(3)	−1481(6)	383(6)	−1705(5)	37(2)
N(4)	3056(6)	3090(5)	173(6)	35(2)
N(5)	4016(6)	2930(6)	2869(6)	39(2)
N(6)	2469(6)	406(6)	3633(6)	41(2)
C(1)	−1757(8)	983(7)	2688(7)	42(2)
C(2)	−2759(8)	1940(8)	1246(8)	51(3)
C(3)	−2615(9)	3049(8)	945(8)	50(3)
C(4)	−2760(7)	3950(7)	−698(7)	37(2)
C(5)	−2770(7)	3726(7)	−1889(7)	39(2)
C(6)	−1495(8)	3453(8)	−2853(7)	44(2)
C(7)	−195(8)	3559(8)	−2599(7)	40(2)
C(8)	632(8)	4141(8)	−2882(7)	45(2)
C(9)	1709(8)	3847(8)	−2367(7)	44(2)
C(10)	1452(8)	3076(8)	−1805(7)	38(2)
C(11)	2134(8)	2416(8)	−1112(7)	45(2)
C(12)	3833(8)	2456(8)	831(7)	43(2)
C(13)	4683(8)	3076(8)	2141(8)	49(3)
C(14)	3464(8)	1730(7)	2817(8)	46(2)
C(15)	3051(8)	1638(7)	3769(7)	41(2)
C(16)	2059(8)	178(8)	4554(8)	50(3)
C(17)	1188(8)	757(8)	4559(8)	42(2)
C(18)	1223(8)	1528(7)	5398(7)	42(2)
C(19)	100(9)	1732(8)	4867(9)	46(2)
C(20)	−542(8)	1091(7)	3746(8)	37(2)

^{a} $U(\text{eq})$ is defined as one-third of the trace of the orthogonalized $\mathbf{U}_{ij}$ tensor.

Table 10. Bond Lengths (Å) and Angles (deg) for **2**

P(1)−O(4)	1.492(6)	N(4)−C(11)	1.518(9)
P(1)−O(3)	1.511(5)	N(5)−C(14)	1.488(10)
P(1)−O(5)	1.594(5)	N(5)−C(13)	1.503(9)
P(1)−O(6)	1.604(5)	N(6)−C(15)	1.504(10)
P(2)−O(8)	1.497(5)	N(6)−C(16)	1.513(9)
P(2)−O(9)	1.522(5)	C(1)−C(20)	1.519(11)
P(2)−O(7)	1.529(5)	C(2)−C(3)	1.504(12)
P(2)−O(6)	1.627(5)	C(4)−C(5)	1.517(10)
O(1)−C(10)	1.367(9)	C(6)−C(7)	1.502(11)
O(1)−C(7)	1.392(10)	C(7)−C(8)	1.328(11)
O(2)−C(20)	1.369(9)	C(8)−C(9)	1.419(11)
O(2)−C(17)	1.381(9)	C(9)−C(10)	1.349(11)
N(1)−C(1)	1.480(10)	C(10)−C(11)	1.478(11)
N(1)−C(2)	1.482(9)	C(12)−C(13)	1.515(11)
N(2)−C(3)	1.484(9)	C(14)−C(15)	1.529(10)
N(2)−C(4)	1.495(9)	C(16)−C(17)	1.485(11)
N(3)−C(6)	1.484(9)	C(17)−C(18)	1.342(11)
N(3)−C(5)	1.513(9)	C(18)−C(19)	1.408(11)
N(4)−C(12)	1.497(10)	C(19)−C(20)	1.327(11)

O(4)−P(1)−O(3)	116.2(3)	N(3)−C(5)−C(4)	110.4(6)
O(4)−P(1)−O(5)	109.2(3)	N(3)−C(6)−C(7)	108.7(7)
O(3)−P(1)−O(5)	109.9(3)	C(8)−C(7)−O(1)	109.7(7)
O(4)−P(1)−O(6)	110.9(3)	C(8)−C(7)−C(6)	135.8(9)
O(3)−P(1)−O(6)	105.2(3)	O(1)−C(7)−C(6)	114.5(8)
O(5)−P(1)−O(6)	104.7(3)	C(7)−C(8)−C(9)	108.0(8)
O(8)−P(2)−O(9)	113.9(3)	C(10)−C(9)−C(8)	105.8(8)
O(8)−P(2)−O(7)	113.5(3)	C(9)−C(10)−O(1)	110.9(8)
O(9)−P(2)−O(7)	113.6(3)	C(9)−C(10)−C(11)	134.7(8)
O(8)−P(2)−O(6)	106.6(3)	O(1)−C(10)−C(11)	114.5(8)
O(9)−P(2)−O(6)	107.4(3)	C(10)−C(11)−N(4)	112.4(7)
O(7)−P(2)−O(6)	100.4(3)	N(4)−C(12)−C(13)	112.6(7)
C(10)−O(1)−C(7)	105.6(7)	N(5)−C(13)−C(12)	112.5(7)
C(20)−O(2)−C(17)	105.0(6)	N(5)−C(14)−C(15)	111.1(7)
P(1)−O(6)−P(2)	131.4(3)	N(6)−C(15)−C(14)	107.8(7)
C(1)−N(1)−C(2)	111.2(6)	C(17)−C(16)−N(6)	111.5(7)
C(3)−N(2)−C(4)	114.0(6)	C(18)−C(17)−O(2)	110.2(7)
C(6)−N(3)−C(5)	111.7(6)	C(18)−C(17)−C(16)	133.4(9)
C(12)−N(4)−C(11)	111.9(6)	O(2)−C(17)−C(16)	116.4(8)
C(14)−N(5)−C(13)	113.0(7)	C(17)−C(18)−C(19)	106.6(8)
C(15)−N(6)−C(16)	114.1(7)	C(20)−C(19)−C(18)	107.1(8)
N(1)−C(1)−C(20)	109.9(7)	C(19)−C(20)−O(2)	111.0(8)
N(1)−C(2)−C(3)	109.9(7)	C(19)−C(20)−C(1)	133.5(8)
N(2)−C(3)−C(2)	110.2(7)	O(2)−C(20)−C(1)	115.3(7)
N(2)−C(4)−C(5)	109.1(6)		

Table 11. Distances between H-Bond-Related Atoms (Å)

O(3)···O(5a)	2.60	O(7)···N(5)	2.64
O(5)···O(3a)	2.60	O(8)···N(3)	2.93
O(4)···N(2)	2.70	O(9)···N(1)	2.72
O(7)···N(4)	2.81		

Finally, it should be pointed out that valuable structural information for the complexes can be obtained from X-ray crystallography, keeping in mind that the geometry of complexes in the solid state may be quite different from that in dilute solution. The crystals of the above two binary complexes were isolated from concentrated solution and form polymers in the solid state. However this is not the case in dilute solution, where binary complexes probably exist as discrete molecules.